

Using Gabor Filter Banks and Temporal-Spatial Constraints to Compute 3D Myocardium Strain

Ting Chen, Leon Axel

Abstract—In this paper, we describe a new approach for reconstructing 3D strains in the myocardium using tagged MR images. We first segment the myocardium using a 3D deformable model driven by image gradients and Gabor filter responses. Tags are automatically detected and tracked as deformable thin plates during systole and early diastole. To keep the tracking results more stable and consistent, we use a combination of gradient information, an intensity probabilistic model, the phase information, and a temporal-spatial smoothness constraint. Based on the tag deformation, we compute a dense displacement in the myocardium around both ventricles. The displacements in x -, y -, and z - directions are calculated separately and are combined to form the final displacement maps. We do not use the information outside the segmented surface of the myocardium to avoid displacement errors caused by noises, artifacts, and correlations between different regions in the myocardium. The strain in the myocardium during the heart cycle is derived from the displacement. This method accepts images of either a tag grid or separate horizontal and vertical tag lines as its input. Experimental results on phantom and real data demonstrate good performance of this method in calculating the myocardial strain.

I. INTRODUCTION

Heart disease is the leading cause of death in the developed world. Many heart diseases, such as ischemia and hypertrophy, change heart function and cause abnormal strain distribution in the myocardium. Quantitative analysis of the location and magnitude of the strain abnormality can help the diagnosis and treatment of heart diseases. The strain field is derived from the myocardial displacement, which cannot be imaged well using conventional MR imaging technique. Tagged Magnetic Resonance Imaging (tMRI) [3], however, allows direct detailed imaging of myocardium motion and deformation, which enables the computation of the displacement and strain fields. In tMRI, we generate a family of parallel tagging planes of altered magnetization at end-diastole, e.g., by spatial modulation of magnetization. These tagging planes are perpendicular to the imaging planes and are evenly distributed in space. Intersections of tagging planes and imaging planes appear as dark stripes, which we call tags, in the final MR images. The tag deforms with the underlying myocardium during the heart cycle, until it fades. The deformation of tags reflects the component of myocardial

motion perpendicular to the initial tag planes. Two sets of SA images and one set of LA images, whose tags are initially perpendicular to each other, are needed for the complete analysis of 3D myocardial motion.

tMRI has been extensively used in clinical applications to study the myocardial motion during the heart cycle. However, the tMR image itself cannot be directly used for quantitative analysis. We have to extract the quantitative motion information, i.e., the displacement field, from tMR images before performing the strain calculations. To accurately calculate the strain within the myocardium, we need to solve the following image analysis tasks first:

- 1) Myocardium segmentation in all tMR images to be analyzed;
- 2) Initialization and tracking of tag planes;
- 3) Tag planes (or tag lines) interpolation;
- 4) Merging the x - and y -displacement maps.

There has been much previous research on the automated segmentation of myocardial contours in MR images. However, due to the presence of image artifacts and noise, complex textures and shapes, and especially the intensity inhomogeneity caused by tag lines in the myocardium, the segmentation of tagged myocardium remains a difficult task. Deformable models [2, 4] have been used to address the problem, but their performance has been inconsistent.

In [12], tag lines were automatically initialized using the frequency domain analysis and then were tracked through the heart cycle using phase information on the myocardium. However, when the temporal resolution becomes larger or the deformation magnitude exceeds an upper limit, one or more tags in the image may be skipped by the method. In [7, 8], myocardial motion was tracked using the CINE-HARP (Harmonic phase) method [5]. This method is more robust but it still requires the starting tag location to be close to the final estimation. In [9, 10], a set of control points has been utilized to control the deformation of a B-spline based tag grid model in order to reconstruct the in-plane displacement fields. It is a robust and efficient method when the underlying 'real' displacement map is smooth. However, whenever the complexity of the displacement field increases, this method may end up with an over smoothed motion estimation. Another limitation of the method is that it is a 2D approach, so that there is no explicit way to handle the effect of motion through the image plane. In [13] a 3D motion tracking framework has been proposed, but the method uses spline-based non-rigid registration, which has the same potential problem of over smoothness.

We developed a novel displacement reconstruction

Manuscript submitted April 24th, 2006.

Ting Chen is with the Radiology Department, New York University, New York, NY 10016 USA (phone: 212-263-3318; e-mail: ting.chen@med.nyu.edu).

Leon Axel is with the Radiology Department, New York University, New York, NY 10016 USA (e-mail: leon.axel@med.nyu.edu).

framework in [14]. In this paper, we describe an enhanced version of the framework which integrates Gabor filters and a Temporal-Spatial constraint. This way, we improve the accuracy of the reconstructed displacement map, which leads to a more accurate strain map of the myocardium.

II. METHOD

A. Segmentation

In our framework, we first use a 3D deformable model [11] to segment the epi- and endo-cardial surfaces of the myocardium at an early time phase when the edges and tags are both relatively clear, and then propagate them to other time phases. The model is initialized as four deformable meshes (LV endo-, LV epi-, RV endo-, and RV epi-) [4]. We initially locate the model in the 3D image space by manually picking 8 landmark points in MR images.

To facilitate the convergence of the model to the image data, we use the response of a family of Gabor filters [1], together with the gradient information in the original image, to guide the deformation of the model. The Gabor filter acts as a band-pass filter, with the central spatial frequency of the filter set equal to the local spatial frequency of tags in the image. It has the form of a sinusoidally modulated Gaussian (or a Gaussian-enveloped sinusoid):

$$h(x, y) = g(x, y) \sin(\omega y + \theta) \quad (1)$$

$$\text{where } g(x, y) = \frac{1}{2\pi\sigma_x\sigma_y} \exp\left(-\frac{(x/\sigma_x)^2 + (y/\sigma_y)^2}{2}\right)$$

, ω is the sine wave frequency (in the range $[0.8\omega_{tag}, 1.2\omega_{tag}]$, ω_{tag} is the initial spatial frequency of the tags), θ is the sine wave phase in the range $(0, 2\pi)$, and σ_x and σ_y are the Gaussian width parameters along the x- and y- axes. The change of distance between two tag lines during the heart deformation is less than 20% of the original distance in most cases. By choosing appropriate values for σ_x , σ_y , ω , and θ , the magnitude response of the Gabor filter can be used to remove tags in the myocardium, and the phase response can be used in the following step of tag tracking. Equation (1) removes tags that are perpendicular to the y- axis; a similar formulation can be defined for Gabor filters that remove tags perpendicular to the x- axis.

The process of deforming the model can be divided into two parts: global fitting that adjusts the scale and orientation of the model, and local deformation that guides the model surfaces to the corresponding image features. For the global fitting, we use a Canny edge filter to extract edge points in the Gabor filter's response to the input MR image. The model's global parameters are adjusted by fitting to these edge points. For the local deformation, the gradients in the original image are combined with the edge information in the Gabor filter output to produce a combined external force. The model

deforms under the influence of the new external force and its internal surface constraint. To avoid local minima, we set a node-to-node correspondence between the endo- and epi-meshes. During the local deformation, we first deactivate the epi- mesh so that it only mimics the deformation of the Endo-mesh, without stopping at local edge features. When the Endo- mesh converges with the endocardial surface, we activate the epi- mesh so that it deforms to the epicardial surface using the gradient and Gabor information.

The model combines the shape prior, image information, and the myocardium texture information, so that it has a robust segmentation performance despite image noise, object shape variation, and the complexity of the internal texture.

B. Tag Tracking

We initialize the tag planes at ED (end of Diastole) automatically, using the frequency and intensity information. We can find the optimal location for a group of tag planes when their intersection with image planes has the minimal mean intensity.

At each time point after ED, we first estimate the tag plane intersection with the image plane as:

$$p_i = p_{i-1} + \alpha(p_{i-1} - p_{i-2}) \quad (2)$$

where p_i is the tag's location at the i th time, and α is a constant between 0 and 1 to control the propagation. Assuming this estimation is close to the tag's true location and considering the Gabor filter bank's output of the material point to hold a constant phase during the deformation [8], we use Newton-Raphson iteration to refine the tag's location:

$$p_i^{n+1} = p_i^n - [\nabla \phi(p_i^n)]^{-1} (\phi(p_i^n) - \phi(p_{i-1})) \quad (3)$$

where ϕ is the phase response of the bank of Gabor filters. This creates a set of potential pixels belonging to the tag line. As in [14], we build a statistical intensity model, using the information that the intensity of tags relaxes approximately as an exponential function during the heart cycle.

$$I(i) = A - Be^{-C(i-1)} \quad (4)$$

where i is the index of the cardiac cycle phase; I is the estimated mean intensity of tags; A , B , and C are constants determined by the data. We also compute the standard deviation σ of tag intensity at each time point. Then we build a probabilistic model to decide the probability a pixel belongs to a tag line. We combine the probabilistic model with the temporal estimation at each pixel by dividing the probability by the distance to the estimated tag location. Those pixels whose divided probability still exceeds the threshold (usually 0.5) are accepted as valid data points. We then fit the 3D tag plane to these data points as a deformable mesh. After the 3D deformation, we apply a temporal-spatial constraint to 3D tag plates. We constrain the deformation of tag plates by minimizing the energy:

$$E_{st} = \sum abs[(p_{ijk} - p_{ij-1k})/(p_{ij+1k} - p_{ijk}) - (p_{i-1jk} - p_{i-1j-1k})/(p_{i-1j+1k} - p_{i-1jk})] \quad (5)$$

where P_{ijk} is the location of the k th nodes on the j th tag plate at i th time phase. The energy term keeps the distance between tag plates to be consistent during the tracking process.

C. Displacement Reconstruction

We use the tag tracking results to construct the displacement map. To construct the dense displacement map in image planes, we first refine tag locations (intersection of tag planes and image planes) using a spline model. The tag spline is defined in the pp-form [14],

$$p_j(d) = \sum_{i=1}^k (d - \xi_j)^{k-1} c_{ji} \quad (6)$$

where $\xi_1, \dots, \xi_j, \dots, \xi_{l+1}$ are break points along the spline; c_{ji} are the i th order polynomial coefficients on the j th interval of the spline; j is the index of spline intervals, d is the spline's parameter, and l is the number of intervals. This way, we improve the tag fitting performance close to the myocardium surfaces, since we now estimate the tag location using more reliable information within the myocardium. Intersections of the tag line and the segmented myocardium boundary are end points of tag splines.

We then interpolate between tags, again using splines. The interpolation creates a group of virtual tags, i.e., tag splines whose internal distance is exactly one pixel in the undeformed ED image. Due to the sparseness of tags, there are regions in the myocardium where reliable interpolation results in one or both directions are not available, which means the tag image itself does not contain enough motion information for reconstruction. Under such conditions, we integrate several approaches to get a close approximation to the real displacement field. First, we extrapolate the tag spline model several pixels beyond the myocardium boundary to decrease the region where data for interpolation is unavailable. Second, as in [14] we use a recursive interpolation framework to extend the region of interpolation. Third, after the recursive interpolation, we use a deformable model to estimate the displacement field, based on the known displacement information. We have two assumptions: (1) the initial accepted interpolation result (before extrapolation and recursive interpolation) is a close estimation of the real displacement field; (2) the displacement field has a continuity constraint in the form of thin-plate bending energy. For the displacement field $(u(x, y), v(x, y))$, assumption 1 means that energy

$$\mathcal{E}_1 = \sum_{N_1} (u - u_0)^2 \quad (7)$$

should be minimized, where N_1 is the set of all the pixels

with initial tag interpolation results, and u_0 is the initial interpolation result of displacement in the direction of the x-axis. The equation is defined for the reconstruction of displacement in the x-direction; the equation for the displacement in the y-direction can be defined in a similar form. Assumption 2 means we need to minimize the energy term:

$$\mathcal{E}_2 = \iint_R (u_{xx}^2 + 2u_{xy}^2 + u_{yy}^2) dx dy \quad (8)$$

where R is the region within the myocardial boundary, and u_{xx} , u_{xy} , and u_{yy} are second order derivatives of x-displacement. We estimate the displacement field by minimizing the energy:

$$\mathcal{E} = \lambda_1 \mathcal{E}_1 + \lambda_2 \mathcal{E}_2 \quad (9)$$

where λ_i are empirical weights for the energy components. In [10], a numerical solution for the displacement reconstruction has been given. Noticing that we can use the energy \mathcal{E}_2 to construct the internal energy for a deformable surface constrained by the thin plate bending energy, we reconstruct the displacement field by fitting a deformable surface to the existing displacement values. The nodes on the deformable surface have the initial positions $(x, y, u'(x, y))$, where u' is the displacement field after the recursive interpolation. The deformation process is in the form of a Lagrangian equation:

$$\dot{d} + \mathbf{K}d = f_{ext} \quad (10)$$

where d is the displacement; the stiffness matrix \mathbf{K} is derived from \mathcal{E}_2 ([6] has a detailed explanation about the construction of the stiffness matrix); and magnitude of the external force f_{ext} is defined as the Cartesian distance between the initial interpolation result u_0 and the deformable surface. This way, we can reconstruct the displacement field within each image plane. The displacement field has C^1 continuity. The x- and y-displacements are then combined to construct the final displacement map, since we know the locations of virtual tags intersections in the undeformed image. In Figure 1 we illustrate the segmentation and tracking process.

D. Strain Calculation

The strain is calculated as the derivative of the displacement field in the myocardium. For details, please refer to [4].

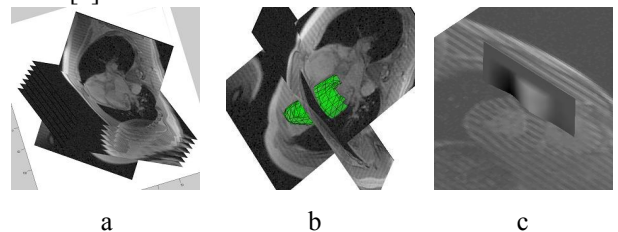
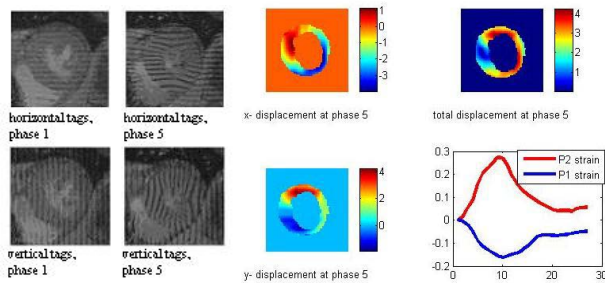


Figure 1: a) is the original 3D data set; b) is the 3D segmentation result; c) is the tag tracking result.

III. EXPERIMENTS AND RESULTS

We show the reconstruction of displacement fields in representative cardiac tMR images (Figure 2). The image set was acquired with a 3T (Siemens Trio) system. The cardiac region of a patient was imaged separately with horizontal and vertical tags. We display on the myocardium the strain map, which is derived directly from the displacement map. The distribution pattern of the myocardium strain matches the prediction of clinical experts. The standard displacement reconstruction time for a 3D data set with 7 slices and 15 time phases is around 10 minutes (Given Gabor filter responses) on a desktop PC with a 2.0GHz CPU and 1G memory.



We validated our method's performance on the phantom by computing the SSD (sum square difference) between the estimation and the predefined displacement field. The final results show that at each pixel the error is 0.13 ± 0.06 pixels with the maximum displacement of 6.2 pixels.

IV. CONCLUSION

We have presented an improved approach to automatically reconstructing the myocardium strain map from tMR data. Our method consists of segmentation, tag tracking, and a reconstruction module. The 3D segmentation algorithm is very fast and needs limited manual input to initialize. The tag tracking is accurate and consistent regardless of the noise level using the phase information from Gabor filters and the temporal-spatial constraint. The final strain map is guaranteed to be smooth. Our approach has a better performance than conventional spline-based displacement reconstruction methods. Our approach is the first to use all the displacement information in a tag line instead of just at the tag intersections, to capture more local displacement details. We expect to test our approach on more patients, in order to build priors for segmentation and motion tracking.

REFERENCES

[1] D. Gabor, "Theory of communication" in Journal of Institution of Electrical Engineers, volume 93, 1946, pp. 429-457.
 [2] M. Kass, A. Witkin, and D. Terzopoulos, "Snakes: Active contour models", volume 1, 1987, pp. 321-331.

[3] L. Axel and L. Dougherty, "MR imaging of motion with spatial modulation of magnetization", in Radiology, volume 171, number 3, 1989, pp. 841-845.
 [4] J. Park, D. Metaxas, and L. Axel, "Volumetric deformable models with parameter functions: A new approach to the 3D motion analysis of the LV from MRI-SPAMM", in proceedings of International Conference on Computer Vision, 1995, pp. 700-705.
 [5] T. S. Denney and J. L. Prince, "Frequency domain performance analysis of Horn and Schunck's optical flow algorithm for deformable motion" *IEEE Trans. Image Processing*, volume 4, number 9, 1995, pp. 1324-1328.
 [6] D. Metaxas, "Physics-based deformable models applications to computer vision, graphics and medical imaging series", Kluwer, Norwell, MA, 02061, USA, 1997.
 [7] N. F. Osman, W. S. Kerwin, E. R. McVeigh, and J. L. Prince, "Cardiac motion tracking using CINE harmonic phase (HARP) magnetic resonance imaging", in Magnetic Resonance in Medicine, volume 42, number 6, 1999, pp. 1048-1060.
 [8] N. F. Osman, E. R. McVeigh, and J. L. Prince, "Imaging heart motion using harmonic phase MRI" *IEEE Trans. Medical Imaging*, volume 19, number 3, 2000, pp. 186-202.
 [9] A. A. Amini, Y. Chen, M. Elayyadi, and P. Radeva, "Tag surface reconstruction and tracking of myocardial beads from SPAMM-MRI with parametric B-spline surfaces", *IEEE Trans. Medical Imaging*, volume 20, number 2, 2001, pp. 94-103.
 [10] Y. Chen and A. A. Amini, "A MAP framework for tag line detection in SPAMM data using Markov random fields on the B-spline solid" *IEEE Trans. Medical Imaging*, vol. 21, number 9, Feb. 2002, pp. 1110-1122.
 [11] T. Chen and D. Metaxas, "Gibbs prior models, marching cubes, and deformable models: A hybrid framework for 3D medical image segmentation". In Proc. of MICCAI 2003, Montreal, vol 2, 703-710.
 [12] Z. Qian, X. Huang, D. Metaxas, and L. Axel, "Robust segmentation of 4D cardiac MRI-tagged images via spatio-temporal propagation", SPIE, Medical Imaging, vol. 5746, pp. 580-591, Apr. 2005.
 [13] R. Chandrasheka, R. Mohiaddin and D. Rueckert, "Comparison of cardiac motion fields from tagged and untagged MR images using non-rigid registration", In Functional Imaging and Modeling of the Heart (FIMH), Lecture Notes in Computer Science, 2005, pp: 425-432.
 [14] L. Axel, T. Chen, and T. Manglik, "Dense myocardium deformation estimation for 2D tagged MRI". FIMH 2005: 446-456